Article

Mechanism of a Strongly Anisotropic Mo–CN–Mn Spin–Spin Coupling in Molecular Magnets Based on the [Mo(CN)] Heptacyanometalate: A New Strategy for Single-Molecule Magnets with High Blocking Temperatures

Vladimir S. Mironov, Liviu F. Chibotaru, and Arnout Ceulemans

J. Am. Chem. Soc., **2003**, 125 (32), 9750-9760• DOI: 10.1021/ja029518o • Publication Date (Web): 22 July 2003

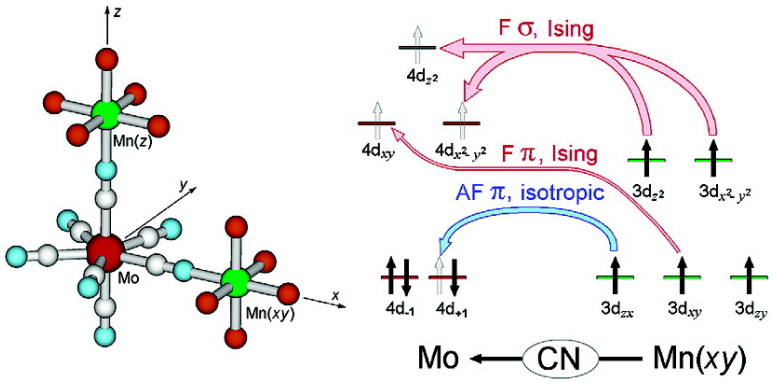

More About This Article

Additional resources and features associated with this article are available within the HTML version:

- Supporting Information
- Links to the 11 articles that cite this article, as of the time of this article download
- Access to high resolution figures
- Links to articles and content related to this article
- Copyright permission to reproduce figures and/or text from this article

View the Full Text HTML

J|A|C|S
ARTICLES
Published on Web 07/22/2003

Mechanism of a Strongly Anisotropic $Mo^{III}-CN-Mn^{II}$ Spin−Spin Coupling in Molecular Magnets Based on the $[Mo(CN)_7]^{4-}$ Heptacyanometalate: A New Strategy for Single-Molecule Magnets with High Blocking Temperatures

Vladimir S. Mironov,*[†,§] Liviu F. Chibotaru,[‡] and Arnout Ceulemans[‡]

Contribution from the Institute of Crystallography Russian Academy of Sciences, Leninskii prosp. 59, 117333 Moscow, Russian Federation and Department of Chemistry, Katholieke Universiteit Leuven, Celestijnenlaan 200F, B-3001 Leuven, Belgium

Received November 28, 2002; E-mail: mirsa@icp.ac.ru

Abstract: Unusual spin coupling between Mo^{III} and Mn^{II} cyano-bridged ions in bimetallic molecular magnets based on the $[Mo^{III}(CN)_7]^{4-}$ heptacyanometalate is analyzed in terms of the superexchange theory. Due to the orbital degeneracy and strong spin−orbit coupling on Mo^{III}, the ground state of the pentagonal-bipyramidal $[Mo^{III}(CN)_7]^{4-}$ complex corresponds to an anisotropic Kramers doublet. Using a specially adapted kinetic exchange model we have shown that the $Mo^{III}-CN-Mn^{II}$ superexchange interaction is extremely anisotropic: it is described by an Ising-like spin Hamiltonian $JS^z_{Mo}\,S^z_{Mn}$ for the apical pairs and by the $J_zS^z_{Mo}\,S^z_{Mn} + J_{xy}(S^x_{Mo}\,S^x_{Mn} + S^y_{Mo}\,S^y_{Mn})$ spin Hamiltonian for the equatorial pairs (in the latter case J_z and J_{xy} can have opposite signs). This anisotropy resulted from an interplay of several Ising-like ($S^z_{Mo}\,S^z_{Mn}$) and isotropic ($\boldsymbol{S}_{Mo}\boldsymbol{S}_{Mn}$) ferro- and antiferromagnetic contributions originating from metal-to-metal electron transfers through the π and σ orbitals of the cyano bridges. The $Mo^{III}-CN-Mn^{II}$ exchange anisotropy is distinct from the anisotropy of the *g*-tensor of $[Mo^{III}(CN)_7]^{4-}$; moreover, there is no correlation between the exchange anisotropy and *g*-tensor anisotropy. We indicate that highly anisotropic spin−spin couplings (such as the Ising-like $JS^z_{Mo}\,S^z_{Mn}$) combined with large exchange parameters represent a very important source of the global magnetic anisotropy of polyatomic molecular magnetic clusters. Since the total spin of such clusters is no longer a good quantum number, the spin spectrum pattern can differ considerably from the conventional scheme described by the zero-field splitting of the isotropic spin of the ground state. As a result, the spin reorientation barrier of the magnetic cluster may be considerably larger. This finding opens a new way in the strategy of designing single-molecule magnets (SMM) with unusually high blocking temperatures. The use of orbitally degenerate complexes with a strong spin−orbit coupling (such as $[Mo^{III}(CN)_7]^{4-}$ or its 5*d* analogues) as building blocks is therefore very promising for these purposes.

Introduction

The interest in single-molecule magnets (SMM) with high blocking temperatures has stimulated extensive studies of magnetic properties of high-nuclearity metal-cyanide clusters.[1,2] Most of the clusters obtained to date are structurally related to the 3-D Prussian blue family compounds containing hexacyanometalates as building blocks. Unfortunately, these systems have generally a low magnetic anisotropy due to the cubic crystal structure and the octahedral symmetry of the $M(CN)_6$ complexes. This does not meet the necessary condition that a pronounced one-center magnetic anisotropy and/or exchange anisotropy between magnetic centers is required for the magnetic cluster to have a high-energy spin reorientation barrier.[2] The use of building blocks with anisotropic magnetic properties is therefore strongly preferable for obtaining good SMM characteristics.

Recently, new cyanide compounds containing the low-symmetry and magnetically anisotropic $[Mo^{III}(CN)_7]^{4-}$ heptacyanometalate and Mn^{II} ions were synthesized and characterized[3]

$Mn_2(H_2O)_5[Mo(CN)_7]\cdot 4H_2O$ **1**

$Mn_2(H_2O)_5[Mo(CN)_7]\cdot 4.75H_2O$ **2**

$K_2Mn_3(H_2O)_6[Mo(CN)_7]\cdot 6H_2O$ **3**

$[N(CH_3)_4]_2[Mn(H_2O)]_3[Mo(CN)_7]_2\cdot 2H_2O$ **4**

These compounds have an extended 3-D (**1**, **2**, and **4**) or 2-D (**3**) crystal structure and order magnetically at 43, 51, 39, and 86 K, respectively.[3] The magnetic behavior of **1**−**4** was found

[†] Institute of Crystallography RAS Moscow.
[‡] Katholieke Universiteit Leuven.
[§] Present address: Department of Chemistry Katholieke Universiteit Leuven Celestijnenlaan 200F, B-3001 Leuven, Belgium. Present e-mail: vladimir.mironov@chem.kuleuven.ac.be.

(1) Ferlay, S.; Mallah, T.; Ouahès, R.; Veillet, P.; Verdaguer, M. *Nature* **1995**, *378*, 701.
(2) (a) Sessoli, R.; Tsai, H.-L.; Schake, A. R.; Wang, S.; Vincent, J. B.; Folting, K.; Gatteschi, D.; Christou, G.; Hendrickson, D. N. *J. Am. Chem. Soc.* **1993**, *115*, 1804. (b) Sessoli, R.; Gatteschi, D.; Caneschi, A.; Novak, M. A. *Nature* **1993**, *365*, 141. (c) Barra, A.-L.; Debrunner, P.; Gatteschi, D.; Schultz, C. E.; Sessoli, R. *Europhys. Lett.* **1996**, *35*, 133. (d) Castro, S. L.; Sun, Z.; Grant, C. M.; Bolinger, J. C.; Hendrickson, D. N.; Christou, G. *J. Am. Chem. Soc.* **1998**, *120*, 2365.

10.1021/ja029518o CCC: $25.00

to be very unusual. The magnetic susceptibility of **1**−**4** is very different along different crystallographic axes, and it is field dependent. The magnetic phase diagrams are complicated and show metamagnetic and spin-reorientation phase transitions. Such a behavior is more typical of 4*f* and 5*f* magnetic compounds rather than of transition metal compounds.

The Mo^{III}−CN−Mn^{II} spin coupling in **1**−**3** was initially interpreted as being ferromagnetic.[3] However, subsequent neutron diffraction experiments revealed that the spin density distribution in compound **3** corresponds to an antiferromagnetic interaction between neighboring Mo^{III} and Mn^{II} centers.[4] This contradiction was qualitatively discussed in ref 3 in terms of a simplified model of the electronic structure of $[Mo(CN)_7]^{4-}$ and competing antiferro- and ferromagnetic interactions between the nearest and next nearest magnetic centers, but an insight into the problem is lacking.

In this paper, we analyze the Mo^{III}−Mn^{II} spin coupling in **1**−**4** using a microscopic model based on the kinetic exchange theory.[5] Due to the orbital degeneracy combined with a strong spin−orbit interaction, the orbital momentum of Mo^{III} in a pentagonal-bipyramidal coordination is unquenched thus resulting in a highly anisotropic *g*-tensor of the ground state of $[Mo(CN)_7]^{4-}$. We show that, apart from the ground state of the Mo^{III} site being magnetically anisotropic, the Mo^{III}−CN−Mn^{II} exchange interaction *itself* is highly anisotropic, which cannot be described by the conventional Heisenberg spin Hamiltonian $-J\boldsymbol{S}_{Mo}\boldsymbol{S}_{Mn}$. In fact, the exchange anisotropy may be so strong that the Mo^{III}−Mn^{II} spin coupling as a whole cannot be even characterized by a definite sign (ferro- or antiferromanetic). We show that the Mo^{III}−CN−Mn^{II} exchange anisotropy is an inherent property of an orbitally degenerate system with a pronounced spin−orbit interaction, which is not related to the single-ion anisotropy of $[Mo(CN)_7]^{4-}$. We also discuss new possibilities in designing single-molecule magnets with high spin reorientation barriers resulting from these findings.

Structure of Mo^{III} −Mn^{II} Cyanometalates and the Ground State of $[Mo(CN)_7]^{4-}$. The structure of the $[Mo(CN)_7]^{4-}$ complex in **1**−**4** corresponds to a distorted seven-coordinate pentagonal bipyramid[3] with almost equal Mo−C distances ranging from 2.11 to 2.19 Å (Figure 1). The degree of the distortion from the ideal D_{5h} bipyramid can be seen from Table 1, which shows the ligand angular coordinates. The molybdenum atom has seven (**1**, **2**) or six (**3**, **4**) −C−N−Mn linkages with the surrounding Mn atoms. The Mn sites have an MnN_4O_2 pseudooctahedral coordination in **1**−**3** with four −N−C−Mo linkages in the equatorial plane and two apical oxygen atoms (in **4**, Mn atoms have an MnN_4O 5-fold coordination[3d]). The 3-D or 2-D extended crystal structures of **1**−**4** are built of the Mo_2Mn_2 cyano-bridged cycles, in which neighboring Mo and Mn atoms share only one cyano group.

In our model approach, we use an idealized geometry of the common Mn(*z*)−Mo−Mn(*xy*) cyano bridged structural unit of **1**−**4** shown in Figure 2. The $[Mo(CN)_7]^{4-}$ heptacyanometalate is assumed to be a regular pentagonal bipyramid of D_{5h} symmetry, and all MnN_4O_2 polyhedra are regarded as octahedra (the fact that in **4** Mn atoms are five-coordinated is not important since the $^6A_{1g}$ ground state of Mn^{II} is spherically symmetric). In this structure, there are only two types of the Mo−CN−Mn linkages, (a) via the apical cyano group along the *z* axis and (b) via the cyano groups in the equatorial *xy* plane. In both cases, the Mo−C−N−Mn group is linear; in case b, the five equatorial ligands of Mo and four equatorial ligands of Mn lie within the same *xy* plane.

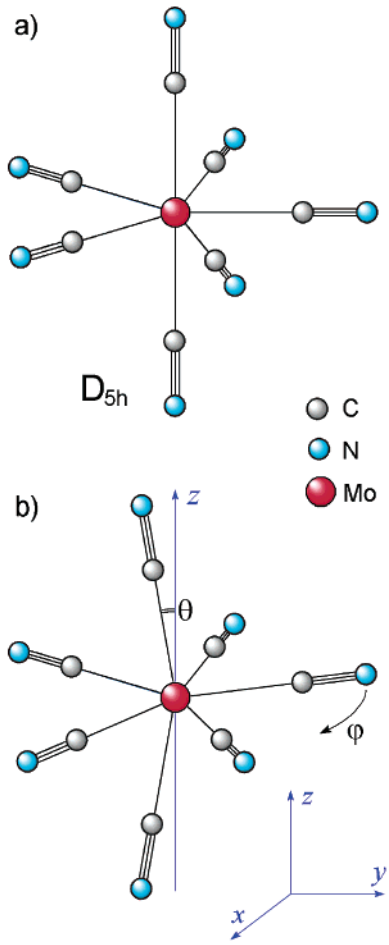

Figure 1. Structure of the $[Mo(CN)_7]^{4-}$ heptacyanometalate: (a) the idealized pentagonal bipyramid (D_{5h} symmetry group) and (b) real distorted bipyramid; the polar (θ) and azimuthal (φ) angles in the regular and distorted complexes are given in Table 1.

Table 1. Polar Coordinates θ and φ of the Cyano Ligands in the D_{5h} Regular Bipyramid and in the Distorted $[Mo(CN)_7]^{4-}$ Complexes in **1**−**4**

θ, degree					φ, degree				
D_{5h}	**1**	**2**	**3**[a]	**4**	D_{5h}	**1**	**2**	**3**[a]	**4**
Apical Ligands									
0	7.0	9.5	9.4	10.2					
180	173.1	170.5	170.7	169.6					
Equatorial Ligands									
90	94.2	74.8	90.1	91.7	0	3.8	-4.5	-2.3	-5.5
90	74.0	94.1	99.3	94.2	72	74.1	67.1	76.6	73.8
90	102.9	91.6	78.7	75.3	144	141.3	145.1	148.7	153.9
90	86.6	85.7	109.9	116.2	216	212.4	220.4	218.4	216.7
90	87.9	111.3	81.5	76.0	288	288.4	292.4	278.6	281.2

[a] According to the recent structural data, in **3** the $[Mo(CN)_7]^{4-}$ complex is less distorted (J. Larionova, private communication).

(3) (a) Larionova, J.; Clérac, R.; Sanchiz, J.; Kahn, O.; Golhen, S.; Ouahab, L. *J. Am. Chem. Soc.* **1998**, *120*, 13088. (b) Larionova, J.; Kahn, O.; Golhen, S.; Ouahab, L.; Clérac, R.; *Inorg. Chem.* **1999**, *38*, 3621. (c) Larionova, J.; Kahn, O.; Golhen, S.; Ouahab, L.; Clérac, R. *J. Am. Chem. Soc.* **1999**, *121*, 3349. (d) Larionova, J.; Clérac, R.; Donnadieu, B.; Guérin, C. *Chem.*−*Eur. J.* **2002**, *8*, 2712.
(4) Stride, A.; Gillon, B.; Goukassov, A.; Larionova, J.; Clérac, R.; Kahn, O. *C. R. Acad. Sci.* **2001**, *24*, 871.
(5) (a) Anderson, P. W. *Phys. Rev.* **1959**, *115*, 2. (b) Anderson, P. W. In *Magnetism*; Rado, G. T., Suhl, H., Eds.; Academic Press: New York, 1963; Vol. 2, Chapter 2.

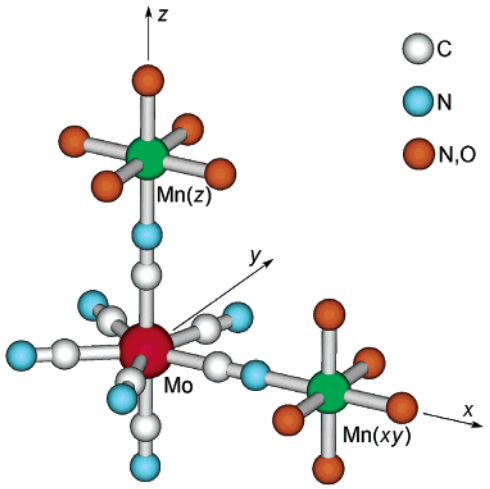

Figure 2. Idealized structure of the Mn(*z*)−Mo−Mn(*xy*) cyano bridged unit of the crystal structure of **1**−**4**. The $[Mo(CN)_7]^{4-}$ complex is the regular pentagonal bipyramid (D_{5h}), and the Mn polyhedra correspond to octahedra (O_h).

Consider the electronic structure of the $[Mo(CN)_7]^{4-}$ heptacyanometalate with the regular D_{5h} geometry. In the crystal field (CF) of D_{5h} symmetry, 4*d* levels of Mo split into the ground orbital doublet (*zx* and *zy* orbitals), the excited doublet (*xy* and $x^2 - y^2$), and the upper singlet (z^2), Figure 3a. These states are characterized by a definite projection of the electron orbital momentum m_l to the *z* axis, $m_l = \pm1$, ±2, and 0, respectively. The 4*d* orbital energies can be calculated in terms of the e_σ and e_π parameters of the angular overlap model (AOM), $E(zx, zy) = {}^9/_2 e_\pi$, $E(xy, x^2 - y^2) = {}^{15}/_8 e_\sigma + {}^5/_2 e_\pi$, and $E(z^2) = {}^{13}/_4 e_\sigma$. Using the values $e_\sigma = 25\,850$ and $e_\pi = 9100$ cm^{-1} obtained from our recent CASPT2 calculations for $Mo(CN)_6^{3-}$,[6] we have $E(zx, zy) = 0$, $E(xy, x^2 - y^2) \approx 30\,000$ and $E(z^2) \approx 43\,000$ cm^{-1}. Three 4*d* electrons of Mo^{III} occupy the two lowest *zx* and *zy* orbitals to form a low-spin $^2\Phi_0(M_L = \pm1)$ orbital doublet (Figure 3b). CF calculations for the $4d^3$ configuration (performed with the $B = 370$ and $C = 1950$ cm^{-1} Racah parameters obtained from CASPT2 calculations[6]) show that this ground state is well isolated since the first excited state lies around 20 000 cm^{-1} (Figure 3b). Under the influence of the spin−orbit interaction on Mo ($\zeta_{4d}\boldsymbol{LS}$), the ground orbitally degenerate $^2\Phi_0(M_L = \pm1)$ state is split into the ground Kramers doublet $\varphi(\pm{}^1/_2)$ and the excited Kramers doublet $\chi(\pm{}^1/_2)$, which are separated by a gap of ζ_{4d}, the spin−orbit coupling constant of Mo, which ranges[7] from 600 to 1000 cm^{-1} (Figure 3c). The two components of the $\varphi(\pm{}^1/_2)$ doublet correspond to the projections $m = -{}^1/_2$ and $m = +{}^1/_2$ of effective spin $S_{Mo} = {}^1/_2$. The corresponding wave functions $\varphi(m)$ have a one-determinant structure, $\varphi(+{}^1/_2) = ||4d_{+1}{}^{\uparrow\downarrow}, 4d_{-1}{}^{\uparrow}||$ and $\varphi(-{}^1/_2) = ||4d_{+1}{}^{\downarrow}, 4d_{-1}{}^{\uparrow\downarrow}||$, where $\uparrow$ and $\downarrow$ denote the $+{}^1/_2$ and $-{}^1/_2$ electron spin wave functions and $4d_{+1} = (4d_{zx} + i4d_{zy})/\sqrt{2}$ and $4d_{-1} = (4d_{zx} - i4d_{zy})/\sqrt{2}$ are complex 4*d* orbitals of Mo with the definite projection of the orbital momentum $m_l = 1$ and $m_l = -1$, respectively (the bottom of Figure 3c). It is important that the total electron spin $S = {}^1/_2$ of Mo^{III} is not a good quantum number since it is coupled with the orbital momentum $M_L = \pm1$ via the spin−orbit interaction. As a result, the *g*-tensor of the ground state is strongly anisotropic, $g_z = 4$ and $g_x = g_y = 0$, so the magnetic moment of $[Mo(CN)_7]^{4-}$ has an Ising-like behavior: it has a maximum value along the *z* axis, while there is no magnetic moment in the equatorial *xy* plane.

In the actual (distorted) $[Mo(CN)_7]^{4-}$ heptacyanometalates, the ground orbital doublet (*xz*, *yz*) is split and thus the anisotropy is reduced (Figure 3d). However, if the splitting δ is smaller than the spin−orbit splitting ζ_{4d}, the above picture would not change much. The splitting δ can be estimated from AOM calculations, $\delta \approx 0.070e_\sigma - 0.215e_\pi$ (**1**), $0.169e_\sigma - 0.384e_\pi$ (**2**), $0.083e_\sigma - 0.157e_\pi$ (**3**), and $0.108e_\sigma - 0.167e_\pi$ (**4**), which is less than or comparable to ζ_{4d} in all compounds **1**−**4**. CF calculations for the $4d^3$ configuration of Mo^{III} in distorted heptacyanometalates in **1**−**4** show that the orbital composition of the wave function of the ground state is rather close to that of the $\varphi(\pm{}^1/_2)$ doublet in the regular D_{5h} complex. The *g*-tensor remains highly anisotropic (g_z ranges from 3.0 to 3.5 and $g_x \approx g_y$ from 0.4 to 1.3), and its principal magnetic axis deviates by less than 20° from the *z* axis, being consistent with the experimental data for the $NaK_3Mo(CN)_7{\cdot}2H_2O$ precursor, $g_z = 3.89$, $g_x = g_y = 1.77$.[8] This indicates that the use of the idealized D_{5h} geometry of $[Mo(CN)_7]^{4-}$ is a good model approach in the analysis of exchange interactions in **1**−**4**.

Mechanism of the Mo^{III}−CN−Mn^{II} Anisotropic Exchange Interactions. The spin coupling in the Mo−CN−Mn cyano bridged pairs (Figure 2) is analyzed in the frame of the Anderson kinetic exchange theory.[5] From this point, it is important to note that specific details of the exchange interaction mechanism in our system are essentially different from those in spin-only exchange systems (including orbitally degenerated systems with a weak spin−orbit coupling). In the latter case, the total spin on magnetic ions is a good quantum number, and thus the resulting effective exchange Hamiltonian always contains the isotropic $\boldsymbol{S}_1\boldsymbol{S}_2$ spin factor; this facilitates considerably the theoretical treatment of the problem. By contrast, in orbitally degenerate systems with a strong spin−orbit coupling, the total spin of magnetic ions is no longer a good quantum number. This situation is typical of lanthanide or actinide ions in solids, and this also takes place in $[Mo(CN)_7]^{4-}$ octacyanometalate, as can be seen from the preceding analysis of its electronic structure. In this case, electronic states of the exchange-coupled pair cannot be classified according to the spin multiplicity, and the resulting spin Hamiltonian becomes anisotropic. Therefore, the kinetic exchange theory in its conventional form cannot directly be applied to the analysis of non-Heisenberg exchange interactions between the $\varphi(\pm{}^1/_2)$ anisotropic Kramers doublet of Mo^{III} and the true total spin $S_{Mn} = {}^5/_2$ of Mn^{II}. Recently, we have developed a general formalism to describe the kinetic exchange mechanism in systems with a strong spin−orbit interaction, which has been applied to a detailed analysis of the anisotropic Yb^{3+}−Cr^{3+} exchange interaction in the mixed $YbCrBr_9^{3-}$ dimer.[9] Here, we use a simplified version of this theory.

In our approach, the Mo→Mn and Mo←Mn metal-to-metal electron transfers through the bridging ligands are analyzed in

(6) Hendrickx, M. F. A.; Mironov, V. S.; Chibotaru, L F.; Ceulemans, A. *J. Am. Chem. Soc.* **2003**, *125*, 3694.
(7) (a) Dunn, T. M. *Trans. Faraday Soc.* **1961**, *57*, 1441. (b) Kim, D. H.; Lee, M. J. *Bull. Korean Chem. Soc.* **1997**, *18*, 976. (c) Gamelin, D. R.; Güdel, H. U. *J. Phys. Chem. B* **2000**, *104*, 10222.
(8) Hursthouse, M. B.; Malik, K. M. A.; Soares, A. M.; Gibson, J. F.; Griffith, W. P. *Inorg. Chim. Acta* **1980**, *45*, L81.
(9) Mironov, V. S.; Chibotaru, L. F.; Ceulemans, A. *Phys. Rev. B* **2003**, *67*, 014424.

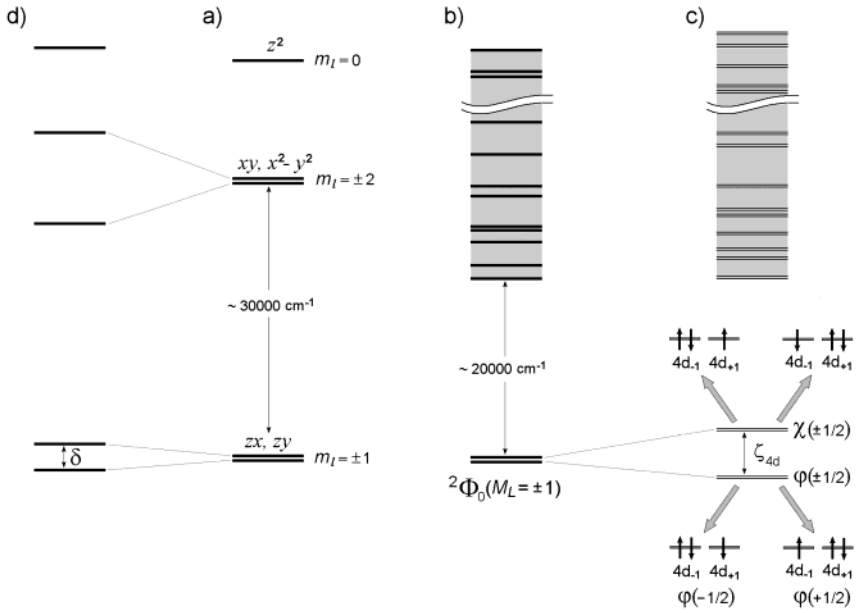

Figure 3. Electronic structure of the $[Mo(CN)_7]^{4-}$ heptacyanometalate: (a) Mo 4*d* orbital energies in a regular D_{5h} pentagonal bipyramid, (b) the energy spectrum of $Mo^{III}(4d^3)$ in the D_{5h} bipyramid without spin−orbit coupling, and (c) the energy spectrum of $Mo^{III}(4d^3)$ in the D_{5h} bipyramid with the spin−orbit coupling. The orbital composition of the ground $\varphi(\pm 1/2)$ and excited $\chi(\pm 1/2)$ Kramers doublets is shown; (d) the splitting of 4*d* orbital energies in distorted $[Mo(CN)_7]^{4-}$ complexes.

terms of individual many-electron states of the $4d^3-3d^5$ basic configuration and $4d^2-3d^6$ and $4d^4-3d^4$ charge-transfer (CT) configurations of a separate Mo−Mn pair, rather than in terms of one-electron states. The wave functions $|m, M_S\rangle$ of the ground level of an $Mo^{III}-Mn^{II}$ pair (which is $2(2S_{Mn} + 1)$-fold degenerate in the absence of exchange interactions) are written as direct antisymmetrized products of the corresponding many-electron wave functions of Mo^{III} and Mn^{II}

$$|m, M_S\rangle = \varphi(m) \otimes {}^6A_{1g}(M_S) \tag{1}$$

where $^6A_{1g}(M_S)$ is the wave function of the $^6A_{1g}$ ground state of Mn^{II} with the spin projection M_S and $m = \pm 1/2$ denotes the components of the ground Kramers doublet of Mo^{III}. Similarly, the wave functions Ψ_n^{CT} of CT many-electron states are written as products of single-ion wave functions of the Mo and Mn centers with one missing or extra electron

$$\Psi_n^{CT}(\text{Mo}\rightarrow\text{Mn}) = \Xi_i^{Mo}(4d^2) \otimes \Xi_j^{Mn}(3d^6) \tag{2}$$

$$\Psi_n^{CT}(\text{Mo}\rightarrow\text{Mn}) = \Xi_i^{Mo}(4d^4) \otimes \Xi_j^{Mn}(3d^4) \tag{3}$$

In this representation, electron transfers are described as $|m, M_S\rangle \rightarrow \Psi_n^{CT} \rightarrow |m', M_S'\rangle$ transitions between the ground and CT many-electron states. Their amplitude is described by the $\langle m, M_S|h|\Psi_n^{CT}\rangle$ matrix elements of the one-electron operator h; the latter is specified by its one-electron matrix elements, that is, transfer integrals $t_{\alpha\beta}$. The effective exchange Hamiltonian H_{eff} is obtained by the projection of CT states onto the space of the $|m, M_S\rangle$ wave functions of the ground level. It is completely defined by the set of the $\langle m, M_S|H_{eff}|m', M_S'\rangle$ matrix elements, which are obtained from the second-order perturbation formula

$$\langle m,M_S|H_{eff}|m',M_S'\rangle = -\sum_{\Psi_n^{CT}} \frac{\langle m,M_S|h|\Psi_n^{CT}\rangle \langle \Psi_n^{CT}|h|m',M_S'\rangle}{E(\Psi_n^{CT})} \tag{4}$$

where the sum runs over all Ψ_n^{CT} states of an Mo−Mn pair resulting from the Mo→Mn and Mo←Mn electron transfers and $E(\Psi_n^{CT})$ is the corresponding CT energy. As shown below, the H_{eff} operator can easily be transformed to the conventional spin Hamiltonian.

Note that many-electron-wave functions were used in many theoretical works on the superexchange interaction in spin-only transition metal dimers[10] and in orbitally degenerate dimers without spin−orbit coupling.[11] However, anisotropic exchange interactions were not analyzed in this frame, and no attempts to calculate anisotropic spin Hamiltonians were made. Our approach represents therefore an extension of the many-electron formalism to the case of orbitally degenerate systems with a strong spin−orbit coupling.

There are some selection rules for nonzero transfer parameters $t_{\alpha\beta}$ connecting the $4d_\alpha$ and $3d_\beta$ metal orbitals for the apical and equatorial Mo−CN−Mn pairs, which are summarized in Table 2. All $t_{\alpha\beta}$ quantities are expressed via the t_π and t_σ transfer parameters describing the electron transfers between 4*d* and 3*d* orbitals through the π and σ orbitals of the cyano bridge (Figure 4). Note that for the two lowest 4*d* orbitals of Mo we use the $4d_{\pm 1}$ complex orbitals rather than the $4d_{zx}$ and $4d_{zy}$ real orbitals (and similarly for the Mn(*z*) $3d_{\pm 1}$ orbitals).

We first consider the apical Mo−CN−Mn(*z*) pair (Figure 2). To illustrate the origin of the anisotropic exchange, consider, for example, the electron transfers for the $|m = -1/2, M_S = 5/2\rangle$ state of the ground level (Figure 5). According to the selection rules for the $t_{\alpha\beta}$ transfer parameters (Table 2), there are two Mo→Mn(*z*) electron transfers of the π type, $4d_{+1}\downarrow \rightarrow 3d_{+1}\downarrow$ and $4d_{-1}\downarrow \rightarrow 3d_{-1}\downarrow$, of which the $4d_{+1}\downarrow \rightarrow 3d_{+1}\downarrow$ transfer between

(10) (a) Glerup, J. *Acta Chem. Scand.* **1972**, *26*, 3775. (b) Weihe, H.; Güdel, H. U. *Inorg. Chem.* **1997**, *36*, 3632.
(11) (a) Weihe, H.; Güdel, H. U. *Chem. Phys. Lett.* **1996**, *261*, 123. (b) Ceulemans, A.; Chibotaru, L. F.; Heylen, G. A.; Pierloot, K.; Vanquickenborne, L. G. *Chem. Rev.* **2000**, *100*, 787. (c) Borras-Almenar, J. J.; Clemente-Juan, J. M.; Coronado, E.; Palii, A. V.; Tsukerblat, B. S. *J. Phys. Chem.* **1998**, *102A* , 200.

Table 2. Nonzero $t_{\alpha\beta}$ Transfer Parameters Connecting Mo $4d_\alpha$ and Mn $3d_\beta$ Orbitals in the Apical (z) and Equatorial (xy) Mo−CN−Mn Pairs (Figure 2)

$4d_\alpha$	$3d_\beta$	$t_{\alpha\beta}$
	Mo−CN−Mn(z) Pair	
$4d_{+1}$	$3d_{+1}$	t_π
$4d_{-1}$	$3d_{-1}$	t_π
$4d_{z^2}$	$3d_{z^2}$	t_σ
	Mo−CN−Mn(xy) Pair	
$4d_{+1}$	$3d_{zx}$	$t_\pi/\sqrt{2}$
$4d_{-1}$	$3d_{zx}$	$t_\pi/\sqrt{2}$
$4d_{xy}$	$3d_{xy}$	t_π
$4d_{z^2}$	$3d_{z^2}$	$t_\sigma/4$
$4d_{z^2}$	$3d_{x^2-y^2}$	$-t_\sigma\sqrt{3}/4$
$4d_{x^2-y^2}$	$3d_{z^2}$	$-t_\sigma\sqrt{3}/4$
$4d_{x^2-y^2}$	$3d_{x^2-y^2}$	$3t_\sigma/4$

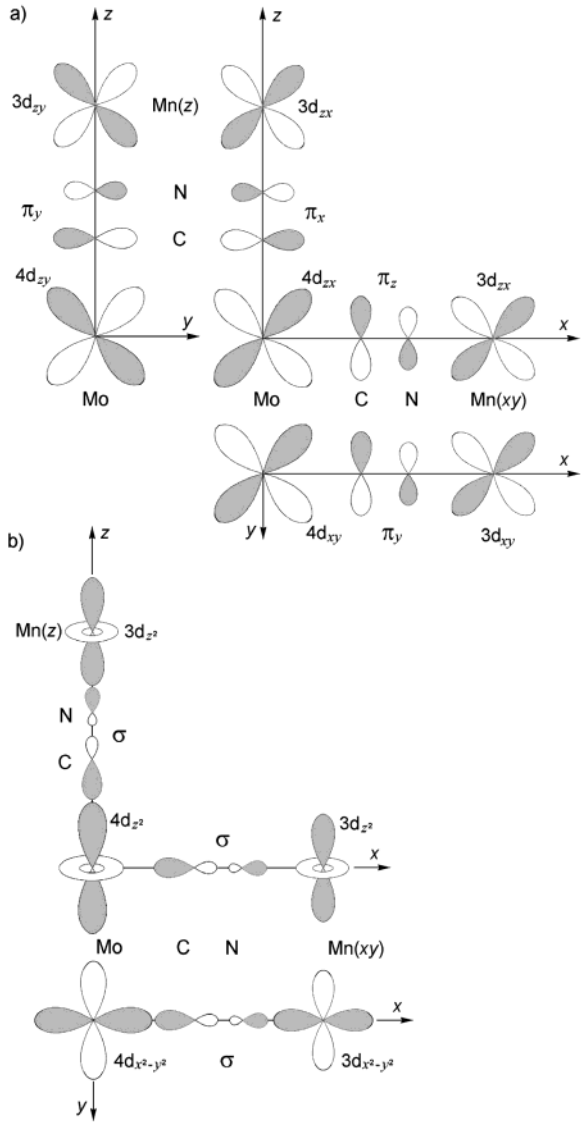

Figure 4. Interactions of Mo 4d orbitals and Mn 3d orbitals through the π (a) and σ (b) orbitals of the cyano bridges in the apical Mo−CN−Mn(z) and equatorial Mo−CN−Mn(xy) pairs. The corresponding transfer parameters are expressed via the t_π and t_σ parameters (Table 2).

two half-filled orbitals is more important (Figure 5a, the blue arrow). When an electron occupies the $3d_{+1}$ orbital, the $^6A_{1g}(M_S = {}^5/_2)$ state of Mn^{II} is transformed to the $^5T_{2g}(3d^6, 3d_{+1}\uparrow\downarrow, M =$

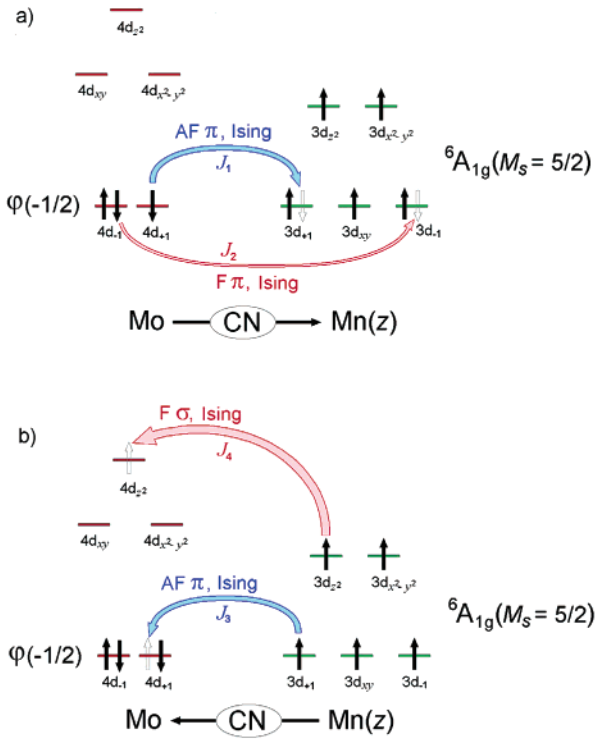

Figure 5. Ferro- (F, pink arrows) and antiferromagnetic (AF, blue arrows) contributions to the spin coupling in the apical Mn−CN−Mo(z) pair resulting from the (a) Mo→Mn(z) and (b) Mo←Mn(z) π and σ electron transfers. All contributions are strongly anisotropic and have an Ising-like character, $J_n S^z_{Mo} S^z_{Mn}$.

2) state corresponding to the component of the $^5T_{2g}(3d^6)$ triply degenerate level with the doubly occupied $3d_{+1}$ orbital and the total spin projection $M = 2$.

The wave function of this CT state is written as $\Psi^{CT}(4d_{-1}\uparrow\downarrow, 3d_{+1}\uparrow\downarrow, M = 2) = ||4d_{-1}\uparrow\downarrow|| \otimes {}^5T_{2g}(3d,^6\, 3d_{+1}\uparrow\downarrow, M = 2)$ and the matrix element is given by

$$\langle -{}^1/_2, {}^5/_2\, |h|\, \Psi^{CT}(4d_{-1}\uparrow\downarrow, 3d_{+1}\uparrow\downarrow, M = 2)\rangle = t_\pi \qquad (5)$$

Transfers between other $|-{}^1/_2, M_S\rangle$ and CT states can also occur. In this case, nonzero matrix elements can only appear if $M = M_S - {}^1/_2$. The CT wave function is now written as $\Psi^{CT}(4d_{-1}\uparrow\downarrow, 3d_{+1}\uparrow\downarrow, M_S - {}^1/_2) = ||4d_{-1}\uparrow\downarrow|| \otimes {}^5T_{2g}(3d^6, 3d_{+1}\uparrow\downarrow, M = M_S - {}^1/_2)$, so we have

$$\langle -{}^1/_2, M_S|h|\Psi^{CT}(4d_{-1}\uparrow\downarrow, 3d_{+1}\uparrow\downarrow, M_S - {}^1/_2)\rangle = \frac{t_\pi}{\sqrt{5}}\sqrt{5/2 + M_S} \qquad (6)$$

Calculations for the $|+{}^1/_2, M_S\rangle$ states are similar. In this case, we obtain

$$\langle +{}^1/_2, M_S|h|\Psi^{CT}(4d_{+1}\uparrow\downarrow, 3d_{-1}\uparrow\downarrow, M_S + {}^1/_2)\rangle = \frac{t_\pi}{\sqrt{5}}\sqrt{5/2 - M_S} \qquad (7)$$

It is important that none of the CT states have nonzero matrix elements simultaneously with the $|-{}^1/_2, M_S\rangle$ and $|+{}^1/_2, M_S'\rangle$ states. This means that only diagonal matrix elements $\langle m, M_S|H_{eff}|m', M_S'\rangle$ with $m = m'$ and $M_S = M_S'$ can appear

from π electron transfers between the half-filled metal orbitals. Then, from eqs 4, 6, and 7, we arrive at

$$\langle -^1/_2, M_S|H_{\text{eff}}| -^1/_2, M_S\rangle = -\frac{t_\pi^2}{2U_1} - \frac{t_\pi^2}{5U_1}M_S \qquad (8)$$

$$\langle +^1/_2, M_S|H_{\text{eff}}| +^1/_2, M_S\rangle = -\frac{t_\pi^2}{2U_1} + \frac{t_\pi^2}{5U_1}M_S \qquad (9)$$

where U_1 is the Mo→Mn CT energy. These equations can be combined as

$$\langle m, M_S\,|H_{\text{eff}}|\, m, M_S\rangle = -\frac{t_\pi^2}{2U_1} + \frac{2t_\pi^2}{5U_1}mM_S \qquad (10)$$

The effective operator of these matrix elements corresponds to the spin Hamiltonian

$$-\frac{t_\pi^2}{2U_1} + \frac{2t_\pi^2}{5U_1}S^z_{\text{Mo}}\,S^z_{\text{Mn}} \qquad (11)$$

where the spin operators for Mo and Mn are defined by

$$S^z_{\text{Mo}}\,\varphi(m) = m\varphi(m) \qquad (12a)$$

$$S^+_{\text{Mo}}\,\varphi(m) = \sqrt{3/4 - m(m+1)}\,\varphi(m+1) \qquad (12b)$$

$$S^-_{\text{Mo}}\,\varphi(m) = \sqrt{3/4 - m(m-1)}\,\varphi(m-1) \qquad (12c)$$

$$S^z_{\text{Mn}}\,{}^6A_{1g}(M_S) = M_S\,{}^6A_{1g}(M_S) \qquad (12d)$$

$$S^+_{\text{Mn}}\,{}^6A_{1g}(M_S) = \sqrt{(S_{\text{Mn}} - M_S)(S_{\text{Mn}} + M_S + 1)}\,{}^6A_{1g}(M_S + 1) \qquad (12e)$$

$$S^-_{\text{Mn}}\,{}^6A_{1g}(M_S) = \sqrt{(S_{\text{Mn}} + M_S)(S_{\text{Mn}} - M_S + 1)}\,{}^6A_{1g}(M_S - 1) \qquad (12f)$$

The first term in eq 11 represents the spin-independent constant. From the second one, we obtain that the Mo→Mn(z) π electron transfer between half-filled 4*d* and 3*d* orbitals (Figure 5a, the blue arrow) gives rise to an antiferromagnetic Ising spin Hamiltonian $-J_1S^z_{\text{Mo}}\,S^z_{\text{Mn}}$ with the exchange parameter

$$J_1 = -\frac{2}{5}\frac{t_\pi^2}{U_1} \qquad (13)$$

The sign of the exchange parameter J_1 needs some comments because the magnetic moment on Mo^{III} is related to a fictitious spin $^1/_2$ and not to the true spin. In exchange-coupled pairs with spin-only magnetic centers, positive (ferromagnetic) and negative (antiferromagnetic) exchange parameters correspond to the parallel and antiparallel spin−spin couplings, respectively. In a general case, the sign of the exchange parameters should be defined with respect to orientations of the magnetic moments of interacting centers and not with respect to their spins. This does not change the sign of the exchange parameter for the spin-only case (because the spin is parallel to the magnetic moment) but can reverse the sign for dimers involving ions with a fictitious spin $^1/_2$, in which the *g*-tensor of the ground state may be negative (when the effective spin $^1/_2$ is antiparallel to the magnetic moment). The latter situation was recently analyzed for the $YbCrBr_9^{3-}$ mixed dimer,[9] in which the *g*-tensor of Yb^{3+} is negative. However, in our case, the situation is usual because the effective spin and the magnetic moment on Mo^{III} are parallel to each other (Figure 3c). The negative J_1 parameter thus corresponds to the antiparallel coupling of the magnetic moments of Mo^{III} and Mn^{II} in the ground state of the dimer.

Further analysis shows that the Mo→Mn(z) π electron transfer from doubly occupied 4*d* orbitals to singly occupied 3*d* orbitals (Figure 5a, the pink arrow) results in a ferromagnetic Ising exchange interaction $-J_2S^z_{\text{Mo}}\,S^z_{\text{Mn}}$ with

$$J_2 = +\frac{2}{5}\frac{t_\pi^2}{U_1}\frac{I}{U_1} \qquad (14)$$

where *I* is the intraatomic (Hund) exchange energy on the Mo center. More quantitatively, *I* is the energy separation between low-spin ($S = 0$) and high-spin ($S = 1$) states of the corresponding $4d^2$ or $4d^4$ CT configuration resulting from the loss/gain of one electron from the ground electronic state of the $Mo^{III}(4d^3)$ center. It can be estimated via the Racah parameters as $I \approx 2C + 6B \approx 6000\ \text{cm}^{-1}$, so the I/U_1 ratio is about 0.1−0.15 at a typical CT energy of 5−8 eV. Therefore, the total contribution to the spin coupling resulting from the Mo→Mn π transfers is described by an antiferromagnetic Ising Hamiltonian $-J_{\text{Mo}\rightarrow\text{Mn(z)}}S^z_{\text{Mo}}\,S^z_{\text{Mn}}$ with the exchange parameter $J_{\text{Mo}\rightarrow\text{Mn(z)}} = J_1 + J_2$

$$J_{\text{Mo}\rightarrow\text{Mn(z)}} = -\frac{2}{5}\frac{t_\pi^2}{U_1}\left(1 - \frac{I}{U_1}\right) \qquad (15)$$

Similarly for the Mo←Mn π transfer (Figure 5b, the blue arrow). The CT states are now given by $\Psi^{\text{CT}}([3d_{\pm1}], M) = ||4d_{-1}{}^{\uparrow\downarrow}, 4d_{+1}{}^{\uparrow\downarrow}|| \otimes {}^5T_{2g}(3d^4, [3d_{\pm1}], M)$, where ${}^5T_{2g}(3d^4,[3d_{\pm1}], M)$ is the component of the ${}^5T_{2g}(3d^4)$ state with the empty $3d_{\pm1}$ orbital and the spin projection *M*. This contribution is described by an antiferromagnetic Ising Hamiltonian $-J_3S^z_{\text{Mo}}\,S^z_{\text{Mn}}$ with J_3 being

$$J_3 = -\frac{2}{5}\frac{t_\pi^2}{U_2} \qquad (16)$$

where U_2 is the Mo←Mn CT energy. A σ-type electron transfer from the half-filled $3d_{z^2}$ orbital to the empty $4d_{z^2}$ orbital can also occur (Figure 5b, the bold pink arrow). This contribution corresponds to a ferromagnetic Ising spin Hamiltonian $-J_4S^z_{\text{Mo}}\,S^z_{\text{Mn}}$,

$$J_4 = +\frac{2}{5}\frac{t_\sigma^2}{U_2}\frac{I}{U_2} \qquad (17)$$

where for simplicity we neglected the CF splitting energy in CT states of $Mo(4d^4)$. Thus, collecting the contributions in eqs 15, 16, and 17, we find that the total spin coupling in the Mo−CN−Mn(z) pair is described by a pure Ising Hamiltonian $-JS^z_{\text{Mo}}\,S^z_{\text{Mn}}$ with the exchange parameter

$$J = -\frac{2}{5}\frac{t_\pi^2}{U_1}\left(1 - \frac{I}{U_1}\right) - \frac{2}{5}\frac{t_\pi^2}{U_2} + \frac{2}{5}\frac{t_\sigma^2}{U_2}\frac{I}{U_2} \qquad (18)$$

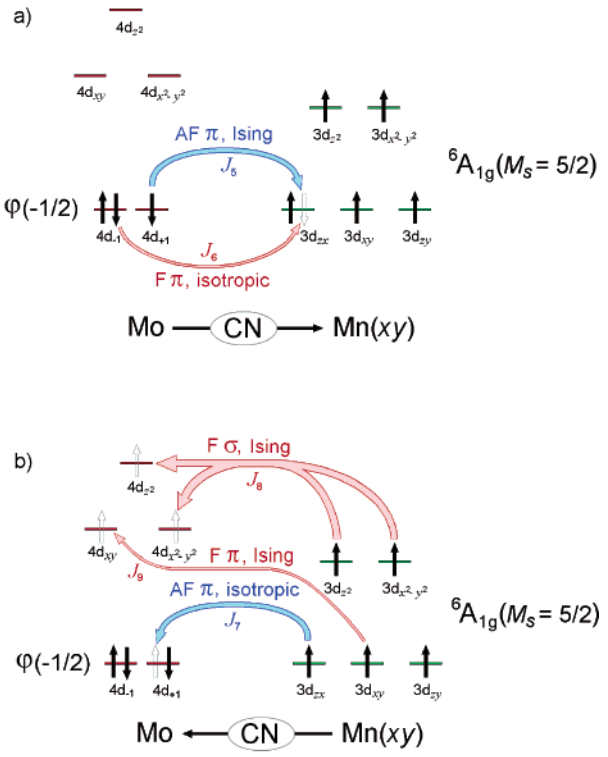

Figure 6. Ising-like and isotropic ferro- (F) and antiferromagnetic (AF) π and σ contributions to the spin coupling in the equatorial Mn−CN−Mo(xy) pair resulting from the (a) Mo→Mn(xy) and (b) Mo←Mn(xy) electron transfers.

Now we turn to the Mo−CN−Mn(xy) equatorial pair. Again, there is an antiferromagnetic Ising-like Mo→Mn(xy) π contribution, $-J_5 S^z_{Mo} S^z_{Mn}$ (Figure 6a, the blue arrow). However, the exchange parameter J_5 is twice smaller than that for the Mo−CN−Mn(z) pair, (J_1, eq 13)

$$J_5 = -\frac{1}{5}\frac{t_\pi^2}{U_1} \tag{19}$$

due to smaller transfer parameters between the $4d_{\pm1}$ and $3d_{zx}$ orbitals (Table 2).

One further difference is that some isotropic π contributions to the spin coupling in the Mo−Mn(xy) pair can appear, J_6 (ferromagnetic, the thin pink arrow in Figure 6a) and J_7 (antiferromagnetic, the blue arrow in Figure 6b). Their origin is best illustrated for the antiferromagnetic contribution J_7. By contrast to the Mo−Mn(z) pair, in which $|m, M_S\rangle \rightarrow \Psi_n^{CT} \rightarrow |m', M_S'\rangle$ transfers occur only for the same initial and final states, in the Mn−Mn(xy) pair, transfers between different $|m, M_S\rangle$ states can appear due to the fact that the Mn(xy) $3d_{zx}$ orbital interacts simultaneously with the Mo $4d_{-1}$ and $4d_{+1}$ orbitals (Table 2). An electron with spin up comes from the $3d_{zx}$ orbital to the half-filled $4d_{+1}$ orbital (Figure 6b, the blue arrow) and then the electron with spin down from the doubly occupied $4d_{-1}$ orbital returns to the vacant $3d_{zx}$ orbital resulting in the $|-^1/_2, {}^5/_2\rangle \rightarrow \Psi_n^{CT} \rightarrow |+^1/_2, {}^3/_2\rangle$ process. The corresponding matrix elements for a given $\Psi^{CT}([3d_{zx}],M_S + {}^1/_2)$ CT state are written as

$$\langle -^1/_2, M_S + 1|h|\Psi^{CT}([3d_{zx}],M_S + {}^1/_2)\rangle = \frac{t_\pi}{\sqrt{10}}\sqrt{S_{Mn} + M_S + 1} \tag{20}$$

$$\langle +^1/_2, M_S|h|\Psi^{CT}([3d_{zx}],M_S + {}^1/_2)\rangle = -\frac{t_\pi}{\sqrt{10}}\sqrt{S_{Mn} - M_S} \tag{21}$$

where the opposite signs in eqs 20 and 21 are due to the different parities of the electron permutations in the determinants. Then, from eq 4 we obtain the $\langle m,M_S \mid H_{eff} \mid m',M_S'\rangle$ nondiagonal matrix elements

$$\langle +^1/_2, M_S|H_{eff}| -^1/_2, M_S + 1\rangle = \frac{t_\pi^2}{10U_2}\sqrt{(S_{Mn} + M_S + 1)(S_{Mn} - M_S)} \tag{22}$$

$$\langle -^1/_2, M_S|H_{eff}| +^1/_2, M_S - 1\rangle = \frac{t_\pi^2}{10U_2}\sqrt{(S_{Mn} - M_S + 1)(S_{Mn} + M_S)} \tag{23}$$

which are rewritten as

$$\langle m,M_S|H_{eff}|m - 1,M_S + 1\rangle = \frac{t_\pi^2}{10U_2}\sqrt{3/4 - m(m-1)}\sqrt{(S_{Mn} - M_S)(S_{Mn} + M_S + 1)} \tag{24}$$

$$\langle m,M_S|H_{eff}|m + 1,M_S - 1\rangle = \frac{t_\pi^2}{10U_2}\sqrt{3/4 - m(m+1)}\sqrt{(S_{Mn} + M_S)(S_{Mn} - M_S + 1)} \tag{25}$$

These matrix elements correspond to a XY spin operator

$$\frac{t_\pi^2}{10U_2}(S^+_{Mo} S^-_{Mn} + S^-_{Mo} S^+_{Mn}) = \frac{t_\pi^2}{5U_2}(S^x_{Mo} S^x_{Mn} + S^y_{Mo} S^y_{Mn}) \tag{26}$$

There are also diagonal matrix elements resulting from the Mo←Mn(xy) π transfers

$$\langle m,M_S|H_{eff}|m,M_S\rangle = -\frac{t_\pi^2}{4U_2} + \frac{t_\pi^2}{5U_2} m M_S \tag{27}$$

which are related to the spin operator

$$-\frac{t_\pi^2}{4U_2} + \frac{t_\pi^2}{5U_2} S^z_{Mo} S^z_{Mn} \tag{28}$$

Combining eqs 26 and 28, we find that spin coupling resulting from the Mo←Mn(xy) π transfers is described by the spin operator

$$-\frac{t_\pi^2}{4U_2} + \frac{t_\pi^2}{5U_2}(S^x_{Mo} S^x_{Mn} + S^y_{Mo} S^y_{Mn} + S^z_{Mo} S^z_{Mn}) = -\frac{t_\pi^2}{4U_2} + \frac{t_\pi^2}{5U_2} \mathbf{S}_{Mo}\mathbf{S}_{Mn} \tag{29}$$

corresponding to the antiferromagnetic isotropic spin coupling $-J_7 \mathbf{S}_{Mo}\mathbf{S}_{Mn}$ with the exchange parameter $J_7 = -t_\pi^2/5U_2$. How-

ever, one should remember that here S_{Mo} measures an axially anisotropic effective spin $^1/_2$ and not the true isotropic spin.

The mechanism for the isotropic ferromagnetic π contribution J_6 (Figure 6a) is treated similarly. It is described by $-J_6 \boldsymbol{S}_{Mo}\boldsymbol{S}_{Mn}$ with the exchange parameter

$$J_6 = +\frac{1}{5}\frac{t_\pi^2}{U_1}\frac{I}{U_1} \tag{30}$$

Again, a considerable ferromagnetic Ising-like contribution $-J_8 S^z_{Mo} S^z_{Mn}$ comes from the Mo←Mn(xy) σ transfers starting from the Mn $3d_{x^2-y^2}$ and $3d_{z^2}$ half-filled orbitals (Figure 6b, the bold pink arrow)

$$J_8 = +\frac{2}{5}\frac{t_\sigma^2}{U_2}\frac{I}{U_2} \tag{31}$$

which is quite similar to that of the Mo←Mn(z) σ transfer, eq 17 (the CF splitting in the Mo($4d^4$) CT states is neglected). In addition, there appears a weaker ferromagnetic Ising-like contribution from the $4d_{xy} \leftarrow 3d_{xy}$ transfers, $-J_9 S^z_{Mo} S^z_{Mn}$ (Figure 6b, the thin pink arrow)

$$J_9 = +\frac{2}{5}\frac{t_\pi^2}{U_2}\frac{I}{U_2} \tag{32}$$

Collecting all Mo→Mn(xy) and Mo←Mn(xy) π and σ contributions and omitting the spin-independent part, we find that the Mo−CN−Mn(xy) exchange interaction is described by a highly anisotropic spin Hamiltonian

$$-J_z S^z_{Mo} S^z_{Mn} - J_{xy}(S^x_{Mo} S^x_{Mn} + S^y_{Mo} S^y_{Mn}) \tag{33}$$

where

$$J_z = \frac{1}{5}\left\{-\frac{t_\pi^2}{U_1}\left(1-\frac{I}{U_1}\right) - \frac{t_\pi^2}{U_2}\left(1-\frac{2I}{U_2}\right) + \frac{2t_\sigma^2}{U_2}\frac{I}{U_2}\right\} \tag{34}$$

$$J_{xy} = -\frac{t_\pi^2}{5}\left(\frac{1}{U_2} - \frac{1}{U_1}\frac{I}{U_1}\right) \tag{35}$$

We find therefore that the spin coupling in the apical and equatorial Mo^{III}−CN−Mn^{II} pairs is strongly anisotropic. The sign and magnitude of the J, J_z, and J_{xy} exchange parameters (eqs 18, 34, and 35) depends on the t_π, t_σ, U_1, U_2, and I microscopic parameters being especially sensitive to the t_σ/t_π ratio. The amplitude of π transfers between cyano-bridged $3d$ ions was analyzed in ref 12, while estimates for σ transfers are lacking. From extended Huckel (EH) calculations for Prussian blue compounds of $3d$ ions, we estimated $t_\pi = 1000-1500$ and $t_\sigma = 2000-3500$ cm^{-1} (with the t_σ/t_π ratio ranging typically from 2 to 3), which give a reasonable agreement between experimental and calculated exchange parameters. Unfortunately, EH calculations poorly reflect the fact that Mo^{III} has diffuse and high-energy $4d$ orbitals giving rise to considerably larger J values in Mo^{III} cyano-bridged compounds as compared to those in related Cr^{III} compounds. For instance, J was found to be -226 cm^{-1} in the $[Mo_2(CN)_{11}]^{5-}$ corner-sharing biocta-

(12) Weihe, H.; Güdel, H. U. *Comments Inorg. Chem.* **2000**, *22*, 75.

hedral dimer of high-spin Mo^{III} [13a] and only -32 cm^{-1} in the structurally similar $[(NH_3)_5Cr^{III}CNCr^{III}(NH_3)_5]^{5+}$ dimer;[13b] in most of the recently obtained Mo^{III} compounds, J is at least twice as large as in their $3d$ counterparts.[13c,d] Thus, in our case t_π and t_σ seem to be larger by a factor of about 1.5 as compared to those estimated from EH calculations with more or less the same t_σ/t_π ratio. From eqs 18, 34, and 35, we can therefore expect that at typical CT energies $U_{1,2} = 40\,000-60\,000$ cm^{-1} the exchange parameters for the Mo^{III}−CN−Mn^{II} pairs with low-spin Mo^{III} can reach a value of many tens of cm^{-1}. Note that this CT energy refers rather to homometallic dimers; for heterometallic dimers, U may be considerably lower thus resulting in even larger exchange parameters. Experimentally, this is consistent with high ordering temperatures in **1**−**4** (i.e., $T_c = 86$ K in **4**[4d] and even more in dehydrated samples[14]).

From these data, we can also estimate the sign of the exchange parameters. For the apical pair, the Ising-type spin coupling (18) is likely antiferromagnetic, since J reverses the sign at a large t_σ/t_π ratio (3 or more), eq 18. For the equatorial pair, J_{xy} is always antiferromagnetic, eq 35; by contrast, J_z becomes ferromagnetic at a reasonable ratio of $t_\sigma/t_\pi \approx 2$ (at $U_1 \approx U_2$ and $I/U_2 \approx 0.15$, eq 34). The same reason was shown to be responsible for the onset of ferromagnetism in Mo^V and Nb^{IV} octacyanometalate bimetallic compounds.[15] Therefore, the J_z and J_{xy} exchange parameters in the Mo−CN−Mn(xy) pair can have opposite signs, $J_z > 0$ and $J_{xy} < 0$. This corresponds to an extreme case of the exchange anisotropy, when the spin coupling as a whole cannot be regarded as ferro- or antiferromagnetic. This situation is very unusual for transition metal compounds, in which anisotropic terms are generally small as compared to the leading isotropic exchange. Previously, opposite signs of the J_z and J_{xy} exchange parameters in the anisotropic spin Hamiltonian were revealed for f ions only: this was observed experimentally in the $YbCrBr_9^{3-}$ mixed $4f-3d$ dimer[16] and in dinuclear rare-earth phthalocyanine complexes.[17]

The origin of the exchange anisotropy and its influence on the global magnetic anisotropy is still poorly understood. It is commonly believed in the literature that the magnetic anisotropy is mostly due to the single-ion anisotropy.[18] We specially emphasize here that generally this is not true. It is important to point out that the exchange anisotropy is not necessarily related to the anisotropy of the g-tensor of the ground state of magnetic ions. These properties are distinct from each other. Although the exchange anisotropy and the anisotropy of the g-tensor of magnetic ions both originate from the spin−orbit coupling, they

(13) (a) Beauvais, L. G.; Long, J. R. *J. Am. Chem. Soc.* **2002**, *124*, 2110. (b) Glerup, J.; Weihe, H. *Acta Chem. Scand.* **1991**, *45*, 444. (c) Sokol, J. J.; Hee, A. G.; Long, J. R. *J. Am. Chem. Soc.* **2002**, *124*, 7656. (d) Shores, M. P.; Sokol, J. J.; Long, J. R. *J. Am. Chem. Soc.* **2002**, *124*, 2279. (e) Berseth, P. A.; Sokol, J. J.; Shores, M. P.; Heinrich, J. L.; Long, J. R. *J. Am. Chem. Soc.* **2000**, *122*, 9655. (f) Mallah, T.; Marvilliers, A.; Riviere, E. *Philos. Trans. R. Soc. London, Ser. A* **1999**, *357*, 3139.

(14) Sutter, J.-P.; Tuna, F.; Tanase, S.; Guionneau, P.; Andruh, M. *VIIIth Int. Conf. Molecule-based Magnets* (Valencia), **2002**, A35.

(15) Chibotaru, L. F.; Mironov, V. S.; Ceulemans, A. *Angew. Chem., Int. Ed.* **2001**, *40*, 4429. In the definition of the exchange Hamiltonian $-2J\boldsymbol{S}_1\boldsymbol{S}_2$, an extra 2 was introduced erroneously, and in eq 6, $(2 - C_\pi)$ should be multiplied by $(\beta_\pi^2 I/(U_2 + \Delta_1)^2)$.

(16) Aebersold, M. A.; Güdel, H. U.; Hauser, A.; Furrer, A.; Blank, H.; Kahn, R. *Phys. Rev. B* **1993**, *48*, 12723.

(17) Maeda, A.; Sugimoto, H. *J. Chem. Soc., Faraday Trans.* **1986**, *2*, 82.

(18) (a) Gatteschi, D.; Sorace, L. *J. Solid State Chem.* **2001**, *159*, 253. (b) Abbati, G. L.; Brunel, L. C.; Casalta, H.; Cornia, A.; Fabretti, A. C.; Gatteschi, D.; Hassan, A. K.; Jansen, A. G. M.; Maniero, A. L.; Pardi, L.; Paulsen, C.; Segre, U. *Chem.−Eur. J.* **2001**, *7*, 1727.

do not correlate to each other. Recently, we have shown that the spin Hamiltonian of the $Yb^{3+}-Cr^{3+}$ superexchange interaction in the $YbCrBr_9^{3-}$ face-sharing bioctahedral dimer is extremely anisotropic despite the fact that both the paramagnetic ions themselves are magnetically isotropic in a local octahedral ligand surrounding.[9] Our theoretical results for $YbCrBr_9^{3-}$ are well consistent with the experimental data.[16] Interestingly, the spin Hamiltonian of the $Yb^{3+}-Cr^{3+}$ pair $H = -J_z S^z_{Yb} S^z_{Cr} - J_\perp(S^x_{Yb} S^x_{Cr} + S^y_{Yb} S^y_{Cr})$ having exchange parameters of opposite sign (antiferromagnetic $J_z = -5.16$ cm^{-1} and ferromagnetic $J_\perp = +4.19$ cm^{-1} [16]) is very similar to that for the equatorial $Mo^{III}-CN-Mn^{II}(xy)$ pair, in which the exchange parameters J_z and J_{xy} can also have opposite signs, eqs 33−35. Previously, strong exchange anisotropy for magnetically isotropic ions was also established theoretically for corner- and edge-sharing bioctahedral f^1-f^1 dimers.[19] In our case, the fact that the $Mo^{III}-CN-Mn^{II}$ exchange anisotropy is not due to the *g*-tensor anisotropy of $[Mo(CN)_7]^{4-}$ is masked by a lower symmetry of the Mo^{III} center.

In actual compounds with distorted $[Mo(CN)_7]^{4-}$ heptacyanometalates, the exchange mechanism is more complicated. The exchange anisotropy decreases but still may be very pronounced, as evidenced from a small value of the ground-state splitting δ, Figure 3d. Obviously, with the present state of the knowledge in this field, a detailed comparison of our theoretical results with the experimental data for **1**−**4** is difficult. Quantitative calculations of anisotropic spin-Hamiltonians for numerous nonequivalent $Mo^{III}-CN-Mn^{II}$ bridges in the actual low-symmetry crystal structures of **1**−**4** are a highly challenging task, which is out of the scope of this paper. In real crystal structures of **1**−**4**, spin Hamiltonians of $Mo^{III}-CN-Mn^{II}$ exchange interactions are complicated due to the appearance of some low-symmetry terms, such as the Dzyaloshinskii−Moriya[20] antisymmetric interaction $\boldsymbol{A}[\boldsymbol{S}_{Mo} \times \boldsymbol{S}_{Mn}]$. As a result, the number of exchange parameters dramatically increases. In this situation, analytical parametric correlations of T_c in **1**−**4** (similar to those performed for cubic Prussian blue compounds of 3*d* elements in ref 12) are generally unreliable. Moreover, even if spin Hamiltonians are known for all Mo−Mn pairs in the unit cell, there still remains a sophisticated problem of determining the magnetic phase diagram of a 2-D or 3-D magnetic lattice involving highly anisotropic spin−spin couplings, such as those in our $Mo^{III}-Mn^{II}$ compounds. Conventional theoretical tools, such as the molecular-field approach, may be inadequate in this case. The magnetic phase diagram of a system with anisotropic exchange interactions is often very complicated (several phase transitions, metamagnetic transitions, etc.), as exemplified by rare-earth and actinide magnetic compounds.[21] Such a behavior is really observed in compounds **1**−**4**. In this context, our theoretical results are well consistent with the anisotropic magnetic properties of **1**−**4**, which cannot be rationalized in terms of the single ion anisotropy only.[3,4] In particular, our results can account for the contradictions in the interpretation of the magnetic properties of **1**−**4**, such as a positive paramagnetic Curie temperature (which is typical for ferromagnets) and an antiferromagnetic ordering revealed from the neutron diffraction experiments.[4]

Therefore, further experimental data on magnetic properties of $Mo^{III}-Mn^{II}$ cyano-bridged compounds are needed for a detailed comparison with the theoretical results. Much more detailed information on the spin−spin coupling in $Mo^{III}-CN-Mn^{II}$ bridges may be obtained from inelastic neutron scattering (INS) experiments for small discrete cyano-bridged clusters (dimers, trimers) containing $[Mo(CN)_7]^{4-}$ heptacyanometalate, rather than for compounds **1**−**4** with 2-D or 3-D extended magnetic lattices. By contrast to magnetization measurements, INS experiments are highly informative in establishing exchange parameters of anisotropic spin Hamiltonians since they determine directly the exchange-split spin energy levels of a discrete magnetic cluster. For instance, the INS technique was employed for determining anisotropic exchange parameters in small Co^{II} magnetic clusters.[22]

Strongly Anisotropic Exchange Interactions: a New Strategy for Single-Molecule Magnets with High Blocking Temperatures. Now we consider the importance of strongly anisotropic exchange interactions in designing molecular magnetic clusters with highly anisotropic magnetic properties. Since the discovery (about a decade ago) of molecular magnetic clusters showing an extremely slow relaxation of magnetization and quantum tunneling effects at low temperatures (single-molecule magnets, SMM), intense investigations of various molecular magnetic clusters with SMM properties have been performed.[2] The interest is stimulated by a potential importance of SMM clusters for high-density data storage and quantum computing. Efficient blocking of magnetization is observed below the blocking temperature, which is closely related to the magnitude of the spin reorientation barrier. The blocking temperature for existing magnetic clusters with SMM properties is still very low (typically, 3 K for the $[Mn_{12}O_{12}(CH_3COO)_{16}(H_2O)_4]\cdot 2CH_3COOH\cdot 4H_2O$ cluster ($Mn_{12}Ac$) having a barrier of about 60 K[23]). The increase of the spin reorientation barrier is therefore the central problem in designing the SMM clusters with higher blocking temperatures.

Generally, there are two distinct aspects of the magnetic anisotropy of a cluster, the anisotropic response to the external magnetic field (the anisotropy of the *g*-tensor and magnetic susceptibility) and the zero-field splitting of the ground spin manifold *S* of the cluster. At present, we shall concentrate on the latter aspect only. The problem of the magnetic anisotropy in molecular magnets has been extensively discussed in recent years.[2,18,22−24] According to the general model, which is most frequently discussed in the literature, exchange interactions between magnetic centers of the cluster are more or less isotropic, so the ground state of the cluster is represented by a definite spin *S*, which is a good quantum number. The degeneracy of the ground spin level is lifted by the macroscopic

(19) Mironov, V. S. *J. Phys.: Condens. Matter* **1996**, *8*, 10551.
(20) (a) Dzyaloshinskii, I. J. *Phys. Chem. Solids* **1958**, *4*, 241. (b) Moriya, T. *Phys. Rev. Lett.* **1960**, *4*, 228. (c) Moriya, T. *Phys. Rev.* **1960**, *120*, 91.
(21) (a) Jensen, J.; Mackintosh, A. R. *Rare Earth Magnetism. Structures and Excitations*; Clarendon Press: Oxford, 1991. (b) Santini P.; Lemanski, R.; Erdos, P. *Adv. Phys.* **1999**, *48*, 537.
(22) (a) Andres, H.; Clemente-Juan, J. M.; Aebersold, M.; Güdel, H. U.; Coronado, E.; Büttner, H.; Kearly, G.; Melero, J.; Burriel, R. *J. Am. Chem. Soc.* **1999**, *121*, 10028. (b) Andres, H.; Clemente-Juan, J. M.; Basler, R.; Aebersold, M.; Güdel, H. U.; Borras-Almenar, J. J.; Gaita, V.; Coronado, E.; Büttner, H.; Janssen, S. *Inorg. Chem.* **2001**, *40*, 1943.
(23) (a) Zhong, Y.; Sarachika, M. P.; Friedman, J. R.; Robinson, R. A.; Kelley, T. M.; Nakotte, H.; Christianson, A. C.; Trouw, F.; Aubin, S. M. J.; Hendrickson, D. N. *J. Appl. Phys.* **1999**, *85*, 5636. (b) Mirebeau, I.; Hennion, M.; Casalta, H.; Andres, H.; Güdel, H. U.; Irodova, A. V.; Caneschi, A. *Phys. Rev. Lett.* **1999**, *83*, 628.
(24) (a) Barra, A.-L.; Brunel, L.-C.; Gatteschi, D.; Pardi, L.; Sessoli, R. *Acc. Chem. Res.* **1998**, *31*, 460. (b) Christou, G.; Gatteschi, D.; Hendrickson, D. N.; Sessoli, R. *MRS Bull.* **2000**, *25*, 66.

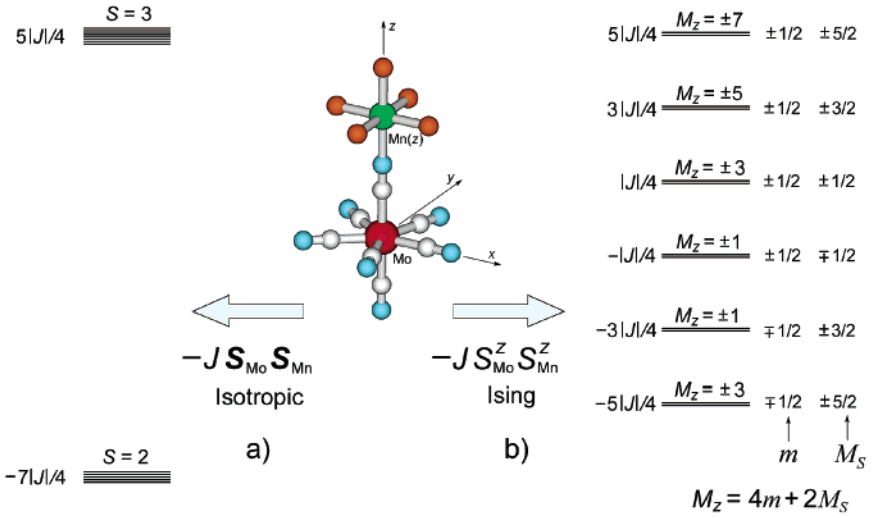

Figure 7. Spin level energies of the apical Mo^{III}−CN−Mn^{II} pair, (a) isotropic antiferromagnetic ($J < 0$) exchange interaction $-J\boldsymbol{S}_{Mo}\boldsymbol{S}_{Mn}$ (hypothetical case) and (b) actual Ising-like antiferromagnetic exchange interaction $-JS^z_{Mo}S^z_{Mn}$. The isotropic exchange gives no splitting of the $S = 2$ ground manifold; a very small splitting can be due to the single-ion zero-field splitting on Mn^{II}. The anisotropic exchange interaction $-JS^z_{Mo}S^z_{Mn}$ gives rise to a doubly degenerate ground state $M_z = \pm 3$ represented by two wave functions $\varphi(-^1/_2) \otimes {}^6A_{1g}(^5/_2)$ ($M_z = +3$) and $\varphi(^1/_2) \otimes {}^6A_{1g}(-^5/_2)$ ($M_z = -3$), where M_z is the projection of the magnetic moment of the Mo^{III}−CN−Mn^{II} pair to the polar axis z ($M_z = g_z(Mo)m + g(Mn)M_S = 4m + 2M_S$). In case b, the dimer represents a single-molecule magnet, since its ground state $M_z = \pm 3$ is separated by a significant energy gap ($|J|/2$, which may reach several tens of cm^{-1}) from the first excited state $M_z = \pm 1$.

zero-field splitting originating from the interplay of the zero-field splitting on the individual magnetic centers. For the axial symmetry, the energy spectrum is described by the DS_z^2 pattern. When D is negative, a double-well potential is formed yielding doubly degenerate a $M = \pm S$ ground state; in this case, the magnetic cluster exhibits SMM properties. The parameter D determines the magnitude of the spin reorientation barrier $|D|S^2$ that separates the $M = +S$ and $M = -S$ states.

The microscopic origin of the global magnetic anisotropy D of SMM clusters is still poorly understood. Most of discussions in the literature revolve around the contributions of the single-ion zero-field splitting and dipolar interactions.[18] Contributions of anisotropic exchange interactions between metal ions to the zero-field splitting of the cluster ions were scarcely considered.

We show that, in a cluster involving strongly anisotropic exchange interactions, the spin spectrum is drastically different from this conventional scheme and the spin reorientation barrier may be considerably larger. This can be best shown for the simplest case of the apical Mo^{III}−$Mn^{II}(z)$ exchange pair, Figures 3 and 7. For this, we compare the spin spectra for two types of the spin coupling in the dimer, hypothetical isotropic spin coupling $-J\boldsymbol{S}_{Mo}\boldsymbol{S}_{Mn}$ (the conventional model), and the actual Ising-like spin $-JS^z_{Mo}S^z_{Mn}$ coupling obtained from our model. For the isotropic exchange, the spin spectrum is described by two levels, $S = 2$ (lower) and $S = 3$ (upper), Figure 7a. The ground level $S = 2$ is not split, so there is no barrier between the $M = 2$ and $M = -2$ states, corresponding to the opposite magnetizations of the cluster. The splitting can come only from the zero-field splitting on the Mn^{II} ion, which is very small ($\sim 10^{-2}$ cm^{-1}). For the antiferromagnetic ($J < 0$) Ising-like spin coupling $-JS^z_{Mo}S^z_{Mn}$, the spectrum is described by the $-JmM_S$ pattern resulting in six doubly degenerate levels, $\pm 5J/4$, $\pm 3J/4$, and $\pm J/4$, Figure 7b. The ground doubly degenerate state $M_z = \pm 3$ is represented by two wave functions $\varphi(-^1/_2) \otimes {}^6A_{1g}(^5/_2)$ and $\varphi(^1/_2) \otimes {}^6A_{1g}(-^5/_2)$, where M_z is the projection of the magnetic moment of the Mo−Mn pair to the polar axis z, Figure 7b. M_z is related to m and M_S by $M_z = g_z(Mo)\,m + g_z(Mn)M_S$, where $g_z(Mo) \approx 4$ and $g_z(Mn) \approx 2$ are z components of the g-tensor of Mo^{III} and Mn^{II}. The ground state is separated by $|J|/2$ from the first excited state $M_z = \pm 1$. Since the total spin of this dimer is not a good quantum number, its ground state cannot be described by a definite spin S. In this case, determining the spin reorientation barrier is not so straightforward as compared to the case of the zero-field split ground spin manifold, DS_z^2. Approximately, the barrier is determined by $|J|$, but its actual value may be even larger. Therefore, according to the above estimates of the exchange parameters, the energy barrier in the apical dimer Mo^{III}−$Mn^{II}(z)$ (Figure 3) has a value of many tens of cm^{-1}. Magnetic properties of this dimer (g-tensor, magnetic susceptibility) are strongly anisotropic. The comparison between two Mo^{III}−Mn^{II} dimers with the isotropic $-J\boldsymbol{S}_{Mo}\boldsymbol{S}_{Mn}$ and Ising-like $-JS^z_{Mo}S^z_{Mn}$ interactions shows that, under the influence of strongly anisotropic exchange interactions, magnetically isotropic transition metal ions, such as Mn^{II}, give a large contribution to the global magnetic anisotropy of the SMM cluster. This contribution vanishes for the isotropic exchange, for which only the zero-field splitting on separate metal ions contribute to the global anisotropy. Therefore, strongly anisotropic exchange interactions are a very important source of the global magnetic anisotropy in molecular magnetic clusters.

We can expect an even more considerable increase in the barrier in going from the Mo^{III}−CN−$Mn^{II}(z)$ dimer to polyatomic Mo^{III}−Mn^{II} cyano-bridged clusters. In this case, the barrier can reach a value of several hundreds of cm^{-1}, even when the size of the cluster remains rather small (about 10 magnetic ions or less). Note that large spin clusters with a high total spin have a pronounced intercluster dipole−dipole interaction, which is unfavorable for obtaining good SMM characteristics. From this point of view, anisotropic exchange interactions ideally are suited for creating high barriers in medium size magnetic clusters. High barriers are more difficult to obtain using the conventional approach, that is, using the single-ion zero-

field splitting only combined with isotropic exchange interactions.[18] Indeed, since the zero-field splitting on 3*d* ions is normally within a few cm^{-1}, about one hundred ions or so are required to obtain a barrier of several hundreds of cm^{-1}; accordingly, the spin of the cluster may be very large ($S \approx 100$) thus resulting in very strong dipole−dipole interactions. This indicates that anisotropic interactions represent a very attractive alternative tool to increase the spin reorientation barrier of SMM clusters. To our knowledge, this subject was not previously discussed in the literature.

Discussion and Conclusions

Our results indicate that the $[Mo(CN)_7]^{4-}$ heptacyanometalate is a very attractive building block for designing cyano-bridged high-nuclearity SMM clusters. Indeed, it has a unique combination of an extremely strong exchange anisotropy and high exchange parameters. Thus, the use of the $[Mo(CN)_7]^{4-}$ complex is a good alternative to the use of lanthanide complexes; the latter, albeit having very strong magnetic anisotropy and high magnetic moment, exhibit generally low exchange parameters (few cm^{-1}). By constructing cyano-bridged clusters containing one or several $[Mo(CN)_7]^{4-}$ complexes and appropriate 3*d* ions (Mn^{II}, Cr^{II}, Cr^{III}, Ni^{II}), one may expect very high spin reorientation barriers (probably, hundreds of cm^{-1}). The spectrum of low-lying spin levels in these clusters may differ considerably from the usual DS_z^2 pattern.[24] In addition, the magnetic moment of such a cluster may be strongly anisotropic and fixed along some axis of the cluster. An interesting combination of unusual magnetic properties and high blocking temperatures can therefore be expected. Presently, only compounds with extended crystal structures were obtained, **1**−**4**. Discrete clusters with the $[Mo(CN)_7]^{4-}$ complexes can be obtained by the use of the blocking ligand technique preventing the formation of extended structures. The efficiency of this approach was recently demonstrated for the synthesis of high-nuclearity metal-cyanide clusters from octahedral $M(CN)_6$ precursors.[13e,f]

The use of related 5*d* cyanometalates instead of $[Mo(CN)_7]^{4-}$ would further increase the exchange coupling and anisotropy. Quite recently, a new $[Re(CN)_7]^{3-}$ building block was obtained, in which $Re^{IV}(5d^3)$ has a slightly distorted pentagonal-bipyramidal coordination and a magnetically anisotropic ground state.[25] $[Re(CN)_7]^{3-}$ represents, therefore, a real 5*d* analogue of $[Mo(CN)_7]^{4-}$. Since the spin−orbit coupling constant of Re is considerably larger (2000−2500 cm^{-1}) than that of Mo (600−1000 cm^{-1}), the ground state of the Re^{IV} heptacyanometalate can remain strongly anisotropic even for more pronounced departures from the strict D_{5h} symmetry.

In summary, the Mo^{III}−CN−Mn^{II} exchange interactions in cyano-bridged bimetallic compounds based on the pentagonal-bipyramidal $[Mo(CN)_7]^{4-}$ heptacyanometalate are analyzed using the Anderson kinetic exchange theory specially adapted for the treatment of anisotropic spin−spin interactions. Our results show that in both the apical and equatorial directions the exchange interaction is strongly anisotropic, mainly due to the orbital degeneracy and strong spin−orbit interaction in the ground state of Mo^{III}. This situation is very unusual for exchange-coupled transition metal ions, in which anisotropic interactions are generally small. This opens a unique possibility for designing SMM with very high spin reorientation barriers and pronounced anisotropic characteristics.

Acknowledgment. Financial support by the Belgian Science Foundation and Flemish Government under the Concerted Action Scheme, the Russian Foundation for Basic Research (Grant No. 01-03-32210), and the INTAS Grant 00-00565 are gratefully acknowledged.

JA029518O

(25) Bennett, M. V.; Long, J. R. *J. Am. Chem. Soc.* **2003**, *125*, 2394.